

Specimen for fracture characterization of material under biaxial stress fields

G. P. Pucillo, M. Grasso, F. Penta and P. Pinto

Department of Mechanics and Energetics, University of Naples Federico II
V. Tecchio-sq. 80, 80125 Naples, Italy. E-mail: gpucillo@unina.it

ABSTRACT. *The simple circular notched specimen was originally proposed by Arcan to characterize the elastic properties of fiber-reinforced composites. Unfortunately, its optimized geometry does not allow to measure with reasonable accuracy both the material shear strength and the conditions of failure under a generic biaxial stress state, since the effects of stress concentration on the fillets of the two V-grooves and on the inner circular edges are responsible of premature fractures due to the uniaxial stress states of the notches edges.*

To improve the performance of this kind of specimen, an extensive FEM analysis has been carried out by a two-dimensional parameterized model, in order to identify those geometries that make possible the fracture to occur in the minimum strength section under the action of a uniform pure shear stress state. Furthermore, the parametric analysis has been extended to the 3D field to define alternative geometries, having variable thickness, that are able to produce with an higher probability material fracture in the minimum strength section.

INTRODUCTION

It is well known that for characterizing accurately the failure properties of engineering interest materials and for formulating the related constitutive and evolution damage laws, the experimental analysis of the effects produced by (at least) biaxial stress states is necessary. Unfortunately, the experimental practices currently adopted for this purpose are quite expensive, due to both the complexity of the testing apparatus and the manufacturing of the test articles, which usually are cruciform or thin-wall cylindrical specimens.

These drawbacks could be overcome if the methodology originally proposed by Arcan [1-3] is adopted. It provides for using either circular notched specimens subjected to diametrical compression or doubly V-notched specimens, also named butterfly shaped specimens, on which testing loads are transferred by means of a special fixture (Arcan fixture). Both kinds of specimen are able to achieve in the region closest to the minimum transversal section a quasi-uniform stress field with principal stresses of opposite sign.

Until now, this type of testing has been used for measuring the elastic shear moduli of linear orthotropic materials [4-8], for the analysis of the non-linear shear response of thick-section pultruded FRP composites beams [9], for the study of mixed or mode II fracture toughness of materials and joints [10-16], or to analyse the strain localization phenomena in cellular materials [17, 18].

By the optimized specimen geometries currently known, neither the material shear strength nor the failure conditions under a generic biaxial stress state can be evaluated with reasonable accuracy, since the stress concentrations on the fillet of the two V-notches and on the inner circular edges are responsible of specimen early fractures due to the uniaxial stresses acting in the notches edges.

Instead, to obtain in the minimum section a pure shear stress distribution as uniform as possible, to which the specimen failure can be ascribed with reasonable confidence, it is preferable to adopt the alternative geometry proposed in [19]. This latter has been defined by means of an extensive FE analysis of a two-dimensional parameterised model of the Arcan specimen, whose geometry was defined by the following parameters: the thickness, t , the radius of the external circular edge, R , the radius of the internal circular edge, r , the semi-opening angle of the notch, θ , the notch fillet radius, ρ , and the half-height, h , that the minimum strength section would have if notch fillet radius was zero (Fig. 1). The original geometry proposed by Arcan is defined by the following values:

$$h/R = 0.1, \quad r/R = 0.2, \quad \rho/R = 0.028, \quad \theta = 45^\circ. \quad (1)$$

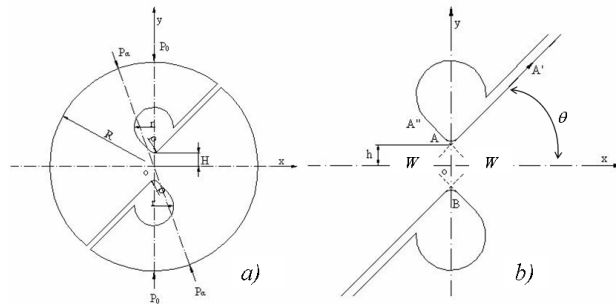


Figure 1 – Original geometry of the Arcan specimen.

Indeed, numerical results obtained in [19] show that both a more uniform shear stress distribution in the minimum strength section and increased chances of failure of the specimen under this latter stress field can be achieved by reducing the semi-height, h , and increasing the inner radius, r , compared to the values proposed by Arcan. When the geometry is so modified, also the stress components σ_x and σ_y in the minimum section are scaled down, while the monoaxial stresses σ acting on the straight edges of the notches are reduced. Moreover, with these new parameters values, the wedge shaped zones of the specimen, W , are more wide (Fig. 1), allowing the adoption of the well

known butterfly shaped specimen [8], which has the advantage of totally avoiding material failures on the circular internal edge.

By increasing the value of θ , the stress peaks close to the notches fillets, due to the abrupt changes of the notch profile curvature, are scaled down, eventually until disappearing. However, the value of θ cannot be increased excessively, because a very high value of θ make strongly not uniform the τ_{xy} distribution in the central part of the minimum section. Anyway, this effect can be balanced with that of the reductions of the notch root radius, ρ , that also cause a reduction of the stress concentration effect on the fillets.

On the basis of previous observations, the following optimal values that define the shape of the specimen have been found:

$$h/R = 0.06, \quad r/R = 0.4, \quad \rho/R = 0.002, \quad \theta = 60^\circ. \quad (2)$$

In the present paper, the study of the Arcan specimen optimal geometry is extended to the 3D field, in order to increase further on the probability that the final fracture takes place in the minimum section of the specimen, since results of numerical analysis till now carried out show that, in any Arcan specimen configuration, it is always possible to find small regions located near the notch roots where the principal stresses field, due to the external load, has a peak (see also Fig. 5).

VARIABLE THICKNESS GEOMETRIES

To reduce the peak stresses near the notch roots, it was thought to increase the specimen thickness in these areas. Stress concentration effects due to the thickness differences between the measure zone and the notch roots areas can be limited by means of two transition zones having “smoothly” variable thickness. To analyse the effect of a variable thickness it is however essential to start from a two-dimensional geometry and gradually increase the thickness at the ends of the minimum section.

The geometry considered in present study is the butterfly one having length and height equal respectively to 200 and 90 mm, notch fillet radius, ρ , equal to 0.5 mm, half-height of the minimum section, h , equal to 15 mm and thickness of 1.6 mm.

The minimum section of the Arcan specimen with variable thickness is shown in Fig. 2: notch roots regions and measure zones have uniform thickness equal to t_1 and t_2 , respectively, and are connected by cylindrical fillets with radius R^* .

3-D 8-node structural solid elements, with 3 translational d.o.f. at each node, have been used to discretize the specimen in the region closest to the minimum section, while for the remaining part of the specimen a more coarse mesh of 3-D 20-node (3 translational d.o.f. per node) tetrahedral elements have been used. Because of the symmetry about the longitudinal plane of the specimen, and the polar-symmetry about the minimum section centroid, only one quarter of the specimen has been considered. Antisymmetric boundary conditions have been imposed to the displacements of nodes

belonging to the minimum section (Fig. 2), while external load was applied on the model by means of a set of constraint equations.

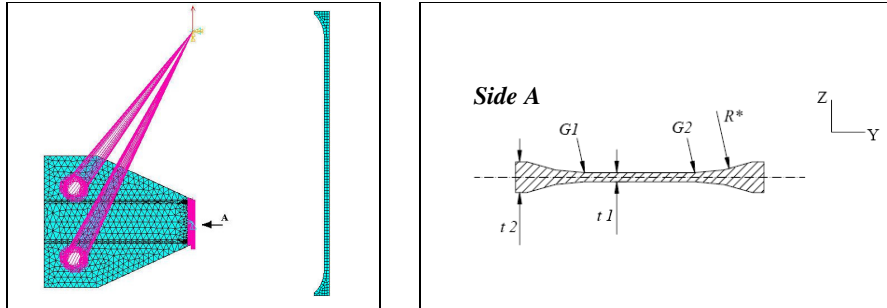


Figure 2 - Left: FEM model of the Arcan specimen; right: minimum section detail.

The analysis have been carried out by varying once the width, $G1-G2$, of the section part having minimum thickness and once the value of the minimum thickness, t_1 (see Fig. 2).

Numerical results of Fig. 3 show that when $G1-G2$ increases, while maintaining fixed the sizes of the parts with maximum thickness (that is decreasing R^* , see Fig. 2), the portion of minimum section under a quasi-uniform shear stress extends and the maximum shear stress gradually assumes smaller values. But the reductions of the radius R^* also produce more severe notch effects in the transition regions.

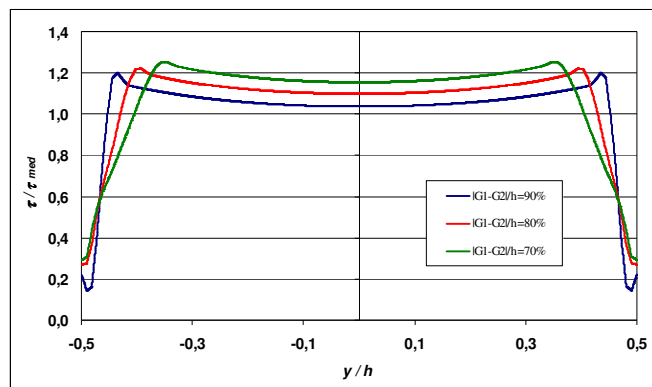


Figure 3 – Shear stress distribution in the minimum section of the modified Arcan specimen for several values of the width $G1-G2$.

An excessive reduction of the minimum thickness, t_1 , has two effects: it leads to a less uniform shear stress distribution on the minimum section (see Fig. 4) and simultaneously it increases the mean value of this distribution. This second effect, for sufficiently small values of t_1 , make the shear stresses in the minimum section more severe than the stress field acting in the notch edges and that indeed is responsible of the

principal drawbacks of both circular and butterfly Arcan specimen. The optimal stress field is achieved by reducing the value of the half-opening angle, θ , as shown in Fig. 6: this reduces the shear stress distribution spikes near the notches and increases the stress field in the central part of the section.

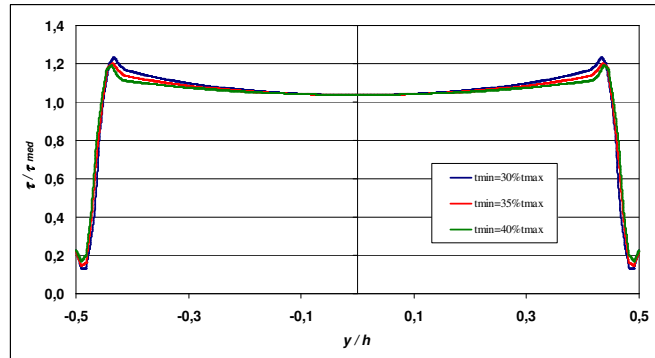


Figure 4 – Shear stress distribution in the minimum section of the modified Arcan specimen for several values of the minimum thickness t_1 .

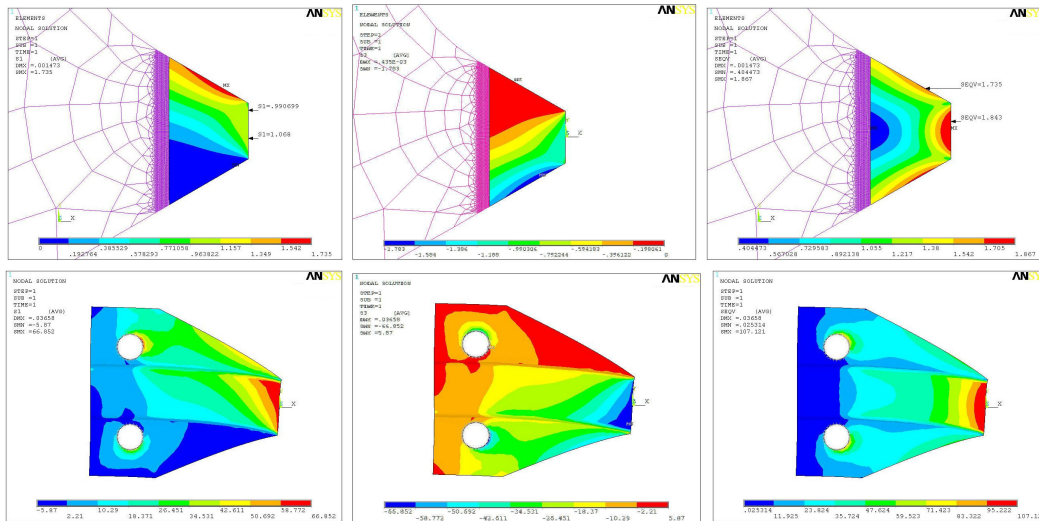


Figure 5 – Stress distributions in the constant (top) and variable (bottom) thickness Arcan specimens. Maximum (left), minimum (center) principal stresses and von Mises equivalent stress (right).

Results from the parametric analysis allow to identify a new optimum 3D geometry, that is characterized by the following values:

$$h/\rho = 30, \quad \theta = 65^\circ, \quad t_{min}/t_{max} = 35\%, \quad G1G2/h = 80\%, \quad (3)$$

and has a bone-shaped minimum section; its geometry is such that the cylindrical transition regions can “work” under a very low stress field. This conclusion is also supported by the diagrams of Fig. 5 where the stress fields acting in both uniform and variable thickness specimens, whose shapes are given by the values of (2) and (3) respectively, are compared.

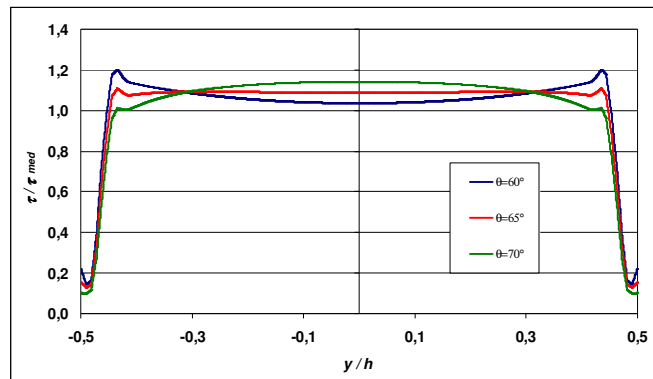


Figure 6 – Shear stress distribution in the minimum section of the modified Arcan specimen for several values of the notch opening semi-angle θ .

BUTTERFLY SHAPED ARCAN SPECIMEN FIXTURE

The proposed testing fixture for the modified Arcan specimen is shown in Fig. 7.

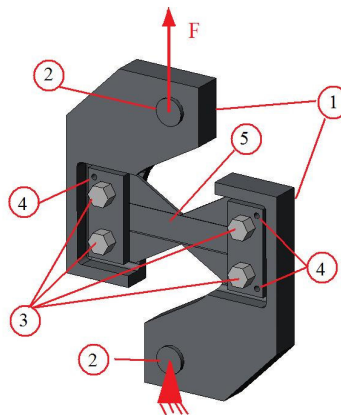


Figure 7 - Arcan testing setup: (1) Arcan fixture, (2) load pins, (3) bolts, (4) positioning pins, (5) specimen.

Essentially, it is composed by two arms, each of them being equipped with: - two holes for the correct positioning of the specimen by means of centering pins; - a couple

of holes for the fastening bolts; - a series of holes positioned on an arc of circumference centered on the centroid of the specimen minimum section. These holes allow to apply on the specimen also loads that are tilted respect to the minimum section.

INVESTIGATIONS FOR BIAXIAL STRESS STATES

In the case of generic biaxial stress states, which can be produced in the measure zone by applying test loads with an angle α not equal to zero, however, the severe notch effect arising in the proximity of the notch root make both the variable thickness specimen and the original Arcan specimen not suitable for the assessment of the material failure properties. A possible solution might be to rotate with an angle equal to α also the central section of the specimen since, as it is shown by the numerical results of Fig. 8, this choice leads to an improvement of the biaxial stress field uniformity in the central part of the minimum strength section. If further modifications in the geometry of the notched region are made, it is however possible, in the Author's opinion, to identify the optimal geometry for each biaxial loading condition to be experimentally analysed.

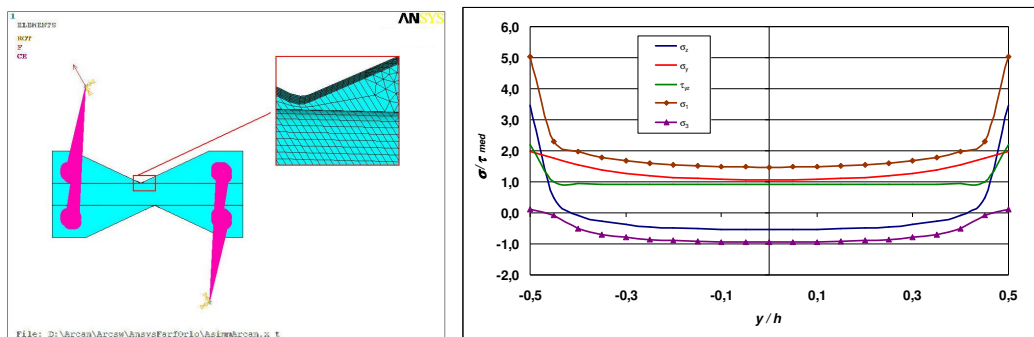


Figure 8 – Left: FEM model. Right: stress field in the minimum section: normal (σ_z), transversal (σ_y), shear (τ_{yz}) and principal stresses (σ_1 , σ_3).

CONCLUSIONS

Modifications of the Arcan specimen geometry, aimed at realizing a uniform pure shear stress distribution, have led to the definition of a bone shaped minimum section. The analysis of the specimen responses, carried out by means of a parameterized FE model, has allowed to optimize the stress distribution in the section of minimum strength. Furthermore, a suitable testing fixture has been proposed that is able to make easier the operations related to the experimental activities scheduled either to validate the model and characterize a material shear behaviour.

Finally, a further modification of the variable thickness geometry has been proposed, to made this latter suitable for studying the material response under a generic biaxial stress state. It is, however, necessary going deeper into the parametrical study in order to identify a correlation between specimen geometry and loading angle that assures both a uniform stress state in the central section of the specimen and the highest probability of specimen failure under this latter stress state.

REFERENCES

1. Goldenberg, N., Arcan, M., Nicolau, E. (1958) *ASTM-STP* **247**, 115-121.
2. Arcan, M., Hashin, Z., Voloshin, A. (1978) *Experimental Mechanics*, **18**, 141-146.
3. Arcan, M. (1984) *Experimental Mechanics*, **24**, 66-67.
4. Voloshin, A., Arcan, M. (1980) *Experimental Mechanics*, **20**, 280-284.
5. Hung, S.C., Liechti, K.M. (1997) *Experimental Mechanics*, **37**, 460-468.
6. Marloff, R.H., Gabrielse, S.E. (1980). In: *Advances in Composite Materials Vol. 1*, pp. 885-899, Bunsell, A.R. et al. (Eds.), Pergamon Press, Elmsfold, New York.
7. Marloff, R.H. (1982) *ASTM-STP* **787**, 34-49.
8. Hung, S.C., Liechti, K.M. (1999) *Journal of Composite Materials*, **33 (14)**, 1288-1317.
9. El-Hajjar, R., Haj-Ali, R. (2004) *Composites: Part B*, **35**, 421-428.
10. Banks-Sills, L., Arcan, M. (1986) *ASTM STP* **905 (17)**, 347-363.
11. Pang, H.L.J, Seetoh, C.W (1997) *Engineering Fracture Mechanics*, **57 (1)**, 57-65.
12. Hallbäck, N. (1997) *International Journal of Fracture*, **87 (4)**, 1573-2673.
13. Jurf, R.A., Pipes, R.B. (1982) *Journal of Composite Materials*, **16**, 386-394.
14. Yoon, S.H., Hong, C.S. (1990) *Experimental Mechanics* **30**, 234-239.
15. Hosseini, S.R., Choupani, N., Gharabaghi, A.R.M. (2008) *International Journal of Mechanical, Industrial and Aerospace Engineering*, **4 (2)**, 241-246.
16. Choupani, N. (2008) *Engineering Fracture Mechanics* **75**, 4363-4382.
17. Doyoyo, M., Wierzbicki, T. (2003) *International Journal of Plasticity* **19**, 1195-1214.
18. Mohr, D., Doyoyo, M. (2003) *Experimental Mechanics* **43 (2)**, 173-182.
19. De Iorio, A., Ianniello, D., Penta, F., Pucillo, G.P. (2002). In *Proceedings of XXXI Convegno Nazionale Associazione Italiana per l'Analisi delle Sollecitazioni (AIAS)*, 18-21 Settembre, Parma, Italy.